Paralic confinement: models and simulations

Emmanuel Frénod, Antoine Rousseau

Paralic Confinement - Models and Simulations

Emmanuel Frénod, Antoine Rousseau

RESEARCH REPORT

N° 7813

November 2011

Project-Teams CALVI and MOISE

ISSN 0249-6399 ISRN INRIA/RR--7813--FR+ENG

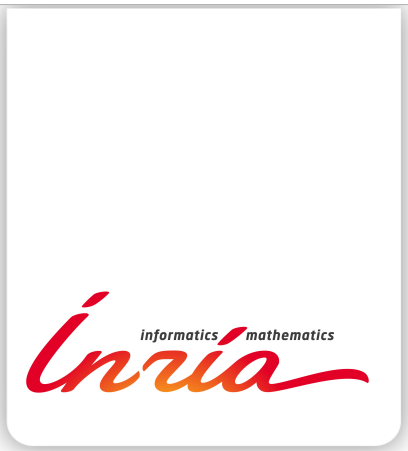

Paralic Confinement - Models and Simulations

Emmanuel Frénod*†, Antoine Rousseau‡

Project-Teams CALVI and MOISE

Research Report n° 7813 — November 2011 — 23 pages

Abstract: This paper deals with the mathematical modelling of confinement of paralic ecosystems. It is based on the recent paper [FG07] that presents a modelling procedure in order to compute the confinement field of a lagoon.
Here, we improve the existing model in order to account for tide oscillations in any kind of geometry such as non-rectangular lagoons with a non-flat bottom. The new model, that relies on PDEs rather than ODEs, is then implemented thanks to the finite element method. Numerical results confirm the feasibility of confinement studies thanks to the introduced model.

Key-words: Mathematical modelling, numerical modelling, partial differential equations, numerical simulations, finite elements, confinement, ecological systems.

* Université Européenne de Bretagne, Lab-STICC (UMR CNRS 3192), Université de Bretagne-Sud, Centre Yves Coppens, Campus de Tohannic, F-56017, Vannes, FRANCE
† INRIA CALVI, Université de Strasbourg, IRMA, 7 rue René Descartes, F-67084 Strasbourg Cedex, FRANCE
‡ INRIA MOISE, Laboratoire Jean Kuntzmann, 51 rue des mathématiques, F-38041 Grenoble Cedex 9, FRANCE

RESEARCH CENTRE
GRENOBLE – RHÔNE-ALPES

Inovallée
655 avenue de l'Europe Montbonnot
38334 Saint Ismier Cedex

Confinement paralique - modèles et simulations

Résumé : Cet article traite de la modélisation mathématique du confinement dans des écosystèmes paraliques. Il se base sur un travail récent [FG07] dans lequel on trouve un modélisation qui permette de simuler le confinement dans des géométries simples.
Ici, on améliore le modèle existant afin de permettre la prise en compte de la marée dans un lagon dont la géométrie est quelconque, avec un fond non nécessairement plat. Notre nouveeau modèle, qui repose sur des équations aux dérivées partielles, est alors implémenté numériquement grâce à la méthode des éléments finis,. Les résultats numériques confirment la faisabilité d'une étude du confinement grâce au modèle proposé.

Mots-clés : Modélisation mathématique, modélisation numérique, équations aux dérivées partielles, équation de transport, simulations numériques, éléments finis, confinement, ecosystèmes.

1 Introduction

The concept of confinement was introduced by Guelorget and Perthuisot [GP83a] in 1983. It has latter been widely used, studied, discussed and tested (see Guélorget and Perthuisot [GP83b, GP83a], Guélorget, Frisoni and Perthuisot [GFP83], Guélorget *et al.* [GGLP90], Ibrahim *et al.* [IGF+85], Debenay, Perthuisot and Colleuil [DPC93], Redois and Debenay [RD96], Barnes [Bar94], Frénod and Goubert [FG07] and Tagliapietra *et al.* [TSG09]) leading to the conclusion that it is a pertinent parameter controlling the features of living benthic population in paralic ecosystems. Benthic species are species living on the seabed and paralic ecosystems are ecosystems encountered in estuaries, lagoons and closed bays.
In all earlier works, no precise definition and no model were given to compute or measure confinement. Yet a biological indicator of confinement, based on species which are specific of each confinement level were existing and well adapted to regions where tide is weak.

Until the paper by Frénod and Goubert [FG07] it was not clear that confinement was also a controlling parameter of tide-influenced paralic ecosystems. In order to help to provide an answer to this question, Frénod and Goubert [FG07] started with the introduction of a definition of confinement usable for modelling purposes:

Definition 1. *The **confinement** value at any point of the lagoon is the time for the sea-water to reach this point.*

The reason why of such a definition is the following: evaporation process on the lagoon surface induces a water flow from the sea to the lagoon far end. All along this flow, water encounters living organisms that take a sample of nutriments. Consequently, water nutriment concentration becomes weaker and weaker, or in other words the environment more and more confined.
For lagoons submitted to forcings that change with time, such as non-constant evaporation rate or tide, the notion of confinement is extended and instantaneous confinement is defined:

Definition 2. *The **instantaneous confinement** is, at a given point of the lagoon and at a given time, the amount of time the water which is at the considered time at the considered point has spent inside the lagoon water mass.*

When those forcings are periodically oscillating, which is the case for tide or periodic evaporation rate, this definition is supplemented (see [FG07]) with the concept of effective confinement:

Definition 3. *The **effective confinement** is the time-average of the instantaneous confinement over its oscillating period.*

Based on those definitions, a model to compute confinement field in a parallelepipedal lagoon was built and implemented. This model was improved thanks to the coupling with tide oscillations, so that confinement in tide-submitted environments could be computed. Moreover developing a simplicist confinement based biological model, it was shown that zonal organization may depend on whether the paralic ecosystem is submitted to tide or not. This advocates for the

fact that confinement is the ecological factor mainly governing benthic species distribution in tided and non-tided paralic environments.

Unfortunately methods and models of Frénod and Goubert [FG07] were only implemented for parallelepipedal lagoons, which is too restrictive in the perspective of testing the accuracy of the concept for real paralic ecosystems.
The goal of this paper is to get rid of this hypothesis by building a model compatible with a lagoon with any shape and any bathymetry, with the restriction that no intertidal zones and no seabed outcrops are taken into account (see Figure 1).

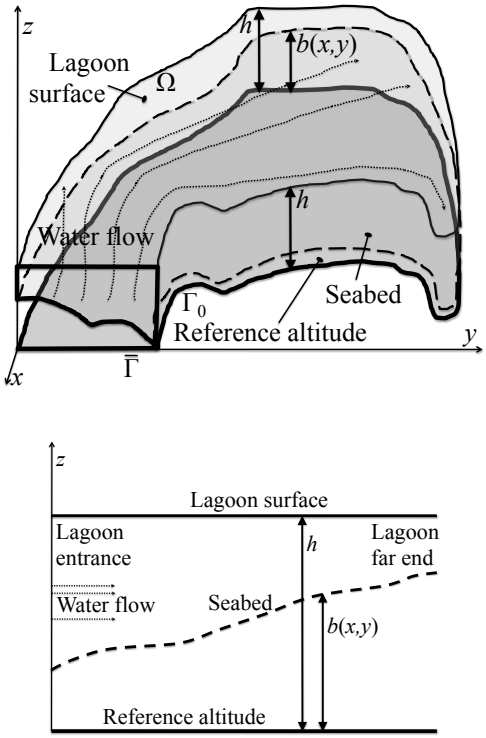

Figure 1: Left: Lagoon geometry; Right: A section of the Lagoon geometry over a line going from the Lagoon entrance to the Lagoon far end.

The essential difference with models of [FG07] is that, here, mathematical models are much less naive and involve Partial Differential Equations (PDEs) instead of Ordinary Differential Equations (ODEs).
The approach we follow to achieve this goal consists, first, in computing the water flow induced by the evaporation process. For this, we follow a simplified fluid dynamics modelling procedure. It consists in translating into PDE language that the evaporated water is immediately replaced by surrounded water. It assumes that, at the time and space scale of interest, the water altitude can be considered as uniform and that the flow has no vortex, because of its slowness. It incorporates a non-uniform seabed such that the water level is, all over the

lagoon, strictly higher than it. The procedure is brought out with a constant evaporation rate and with a variable evaporation rate.
Once the water velocity is computed at any time and in any point in the lagoon, we write the transport equation associated with this field. Among other informations, this transport equation may transport time. Hence, taking definition 1 as the confinement definition, we can compute the confinement field in lagoons without tide and with an evaporation rate that remains positive for all time by solving this equation with ad-hoc boundary conditions.

In a second part, we improve the model in order to account for tide oscillations. To this aim, we consider that a solid shape (fairway) is located at the lagoon entrance (see Figure 2). This fairway communicates with the sea. At any time, the maximum water mass originally located in the lagoon (high tide, during ebbing tide) is actually spread between the lagoon and the fairway. Consequently, in the domain constituted of the union of the lagoon and this fairway, at any time, a varying domain containing the lagoon water mass is defined. Every computation carried out in the case without tide may be done again, with careful adjustments, on this varying domain.

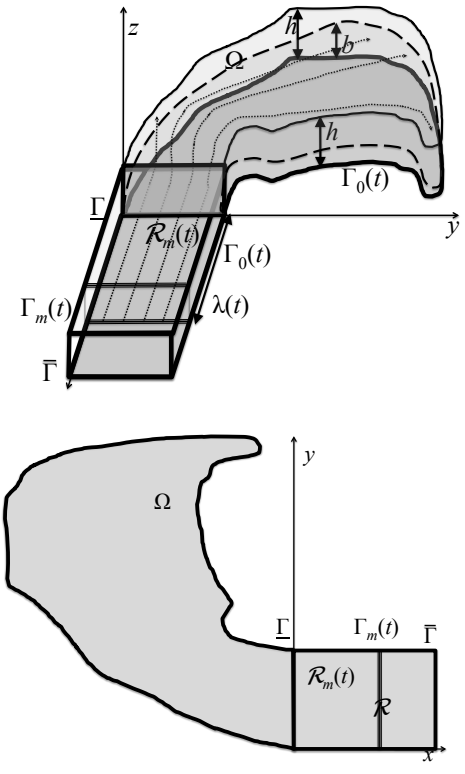

Figure 2: Example of lagoon $\Omega \cup \mathcal{R}$ submitted to tide, with its entrance fairway. Left: 3D view. Right: plan view.

The main objective of this paper is twofold: it consists in building a mathematical model that allows the computation of confinement defined in definitions 1

and 2, but also in implementing a numerical model that provides first numerical results. For the numerical aspects, we use the finite element method, and the numerical results are obtained with Freefem++ (see Hecht, Pironneau and Le Hyaric [HPLH04]).

2 Model for confinement in a lagoon without tide

The goal of this section is to develop a model that will allow us to compute the confinement field within a lagoon with any shape and any bathymetry which is not tide-influenced and which has no seabed outcrop. We start with the description of the lagoon geometry.

2.1 Geometrical model of the lagoon

We consider (see Figure 1) that the lagoon is a cylinder with base a regular, connected and bounded domain $\Omega \subset \mathbb{R}^2$ with boundary $\partial\Omega$. This boundary is shared into $\overline{\Gamma}$ and Γ_0 with $\overline{\Gamma} \cap \Gamma_0 = \emptyset$. Any point in $\overline{\Omega}$ is denoted (x, y). The lagoon seabed is described by a piecewise continuous function $b : \Omega \longrightarrow \mathbb{R}^+$, where $b(x, y)$ represents the bathymetry level at the horizontal position $(x, y) \in \Omega$. The water altitude h is such that $h > \sup_\Omega\{b\}$, exluding outcrops. In summary, the geometrical model of the lagoon writes:

$$\Big\{(x, y, z),\ (x, y) \in \Omega,\ b(x, y) < z < h\Big\}. \tag{1}$$

Figure 3 and equation (25) describe the (smooth) bathymetry that we used in our simulations, but it could be any piecewise continuous function (*e.g.* only defined at mesh points in realistic configurations).

The evaporation process is then modeled by a nonnegative function $\eta = \eta(t, x, y)$ in $L^2(\mathbb{R}^+ \times \Omega)$, which may depend on time and position; η is the space-time density of evaporation. In other words, if $\mathcal{S}$ is a measurable subset of Ω, the water quantity which evaporates through $\mathcal{S}$ over the time interval (t_1, t_2) with $t_1 < t_2$ is:

$$\int_{(t_1,t_2)\times\mathcal{S}} \eta(t, x, y)\ dt\, dx\, dy. \tag{2}$$

Remark 2.1. *In our numerical simulations (see below) we will only consider homogeneous evaporation rates (no space dependency). However, we think that a representative type of evaporation rate could be*

$$\eta(t, x, y) = \eta_1(t)\, \eta_2(x, y), \tag{3}$$

where η_1 would be a (periodic) function of time (possibly accounting for several time scales, from tidal to multi-annual periods), and $\eta_2(x, y)$ a space-attenuation factor, representing the (possible) space variation due to a partly clouded sky, the presence of local vegetation, etc.

2.2 Model for the velocity field

The goal here is to write a PDE, set in Ω, which will allow us to compute the velocity field

$$\vec{v} = \vec{v}(x, y) = \big(v_1(x, y), v_2(x, y)\big) \tag{4}$$

of the water inside the lagoon.

We start with the assumptions concerning this velocity field. The first assumption we make consists in considering that for the phenomenon we want to comprehend, it is enough to consider the mean velocity value over the vertical direction. Moreover, we assume that this mean velocity $\vec{v} = \vec{v}(x, y)$ is purely horizontal. This justifies notation (4). Then we assume that the water movement is solely due to the evaporation process. We also assume that the process is slow enough to consider that the velocity field contains no vortex. Translating this into mathematical terms leads to

$$\nabla \times \vec{v}(x, y) = \frac{\partial v_2}{\partial x}(x, y) - \frac{\partial v_1}{\partial y}(x, y) = 0, \quad \forall (x, y) \in \Omega, \tag{5}$$

where $\nabla\times$ stands for the rotational operator. Equation (5) has the consequence that $\vec{v}$ may expressed as

$$\vec{v}(x, y) = \big(v_1(x, y), v_2(x, y)\big) = \nabla\psi(x, y) = \big(\frac{\partial \psi}{\partial x}(x, y), \frac{\partial \psi}{\partial y} x, y)\big), \quad \forall (x, y) \in \Omega, \tag{6}$$

for a regular function ψ, called the velocity potential.

Now we enter the simplified fluid dynamics modelling procedure. It consists in considering any regular subset $\mathcal{S} \subset \Omega$ and any time interval (t_1, t_2) with $t_1 < t_2$. The amount of water which evaporates through $\mathcal{S}$ over (t_1, t_2), which is given by (2), is simultaneously replaced by water that crosses the lateral surface of the cylinder with base $\mathcal{S}$ and with a lateral surface going from the border $\partial\mathcal{S}$ of $\mathcal{S}$ to the seabed, described by $b(x, y)$, over (t_1, t_2). This lateral surface writes:

$$\mathcal{L} = \Big\{(x, y, z),\ (x, y) \in \partial\mathcal{S},\ b(x, y) < z < h\Big\}. \tag{7}$$

The quantity of water, which is transported by $\vec{v} = \nabla\psi$, entering the cylinder through $\mathcal{L}$ is:

$$-\int_{\mathcal{L}\times(t_1,t_2)} \vec{v} \cdot \vec{n}\, d\mathcal{L}\, dt = -\int_{\partial\mathcal{S}\times\big(b(x,y),h\big)\times(t_1,t_2)} \vec{v} \cdot \vec{n}\, dl\, dz\, dt, \tag{8}$$

where $\vec{n}$ is the unitary vector, orthogonal to $d\mathcal{S}$ and pointing outward $\mathcal{S}$ and where dl is the Lebesgue mesure on $d\mathcal{S}$, $d\mathcal{L}$ being $dldz$. Since $\vec{v}$ is horizontal and independent of z, equation (8) reads

$$-\int_{d\mathcal{S}\times(t_1,t_2)} \big(h - b(x, y)\big)\, \vec{v}(t, x, y) \cdot \vec{n}(x, y)\, dl\, dt. \tag{9}$$

Using Stokes formula, involving the divergence operator, equation (9) reads

$$-\int_{\mathcal{S}\times(t_1,t_2)} \nabla \cdot \big[(h - b(x, y))\vec{v}(t, x, y)\big]\, dx\, dy\, dt. \tag{10}$$

As a consequence of the above statements, quantities defined by equations (2) and (10) must coincide for any $\mathcal{S}$ and any time interval (t_1, t_2). We thus conclude:

$$-\nabla \cdot \big[(h - b)\vec{v}\big](t, x, y) = \eta(t, x, y), \quad \forall t \in \mathbb{R}\ \forall (x, y) \in \Omega, \tag{11}$$

and finally using the definition of ψ:

$$-\nabla\cdot\big[(h-b)\nabla\psi\big](t,x,y)=\eta(t,x,y),\quad \forall t\in\mathbb{R},\ \forall(x,y)\in\Omega. \tag{12}$$

Equation (12) models the water flow dynamics inside the considered lagoon.

To be complete, we need to supplement this equation with boundary conditions that concern the lagoon border. As previously evoked, $\overline{\Gamma}\cup\Gamma_0$ is a partition of the border $\partial\Omega$ of Ω. In what follows, $\vec{n}(x,y)$ stands for the unitary vector orthogonal to $\partial\Omega$ in $(x,y)\in\partial\Omega$ and pointing outward Ω. The boundary $\overline{\Gamma}$ corresponds to the lagoon entrance, which is:

$$\Big\{(x,y,z),\ (x,y)\in\overline{\Gamma},\ b(x,y)<z<h\Big\}. \tag{13}$$

The flux entering the lagoon over a given time interval (t_1,t_2) is

$$\begin{aligned}
&-\int_{\overline{\Gamma}\times[h-b(x,y)]\times(t_1,t_2)}\vec{v}(t,x,y)\cdot\vec{n}(x,y)\ dl\,dz\,dt \\
&\quad=-\int_{\overline{\Gamma}\times[h-b(x,y)]\times(t_1,t_2)}\nabla\psi(t,x,y)\cdot\vec{n}(x,y)\ dl\,dz\,dt \\
&\quad=-\int_{\overline{\Gamma}\times(t_1,t_2)}(h-b(x,y))\frac{\partial\psi}{\partial\vec{n}}(t,x,y)\ dl\,dt,
\end{aligned} \tag{14}$$

where $\partial\psi/\partial n$ is only a notation for $\nabla\psi\cdot\vec{n}$. The boundary Γ_0 is the rest of the lagoon border through which no water crosses, meaning

$$\vec{v}(t,x,y)\cdot\vec{n}(x,y)=\frac{\partial\psi}{\partial\vec{n}}(t,x,y)=0,\quad \forall t\in\mathbb{R},\ \forall(x,y)\in\Gamma_0. \tag{15}$$

The quantity of water evaporating from the lagoon over (t_1,t_2), which writes

$$\int_{\Omega\times(t_1,t_2)}\eta(t,x,y)\quad dx\,dy\,dr, \tag{16}$$

must compensate for the quantity of incoming water over the same period, and which is given by equation (14). Hence

$$\vec{v}(t,x,y)\cdot\vec{n}(x,y)=\frac{\partial\psi}{\partial\vec{n}}(t,x,y)=F_l(t,x,y),\quad \forall t\in\mathbb{R},\ \forall(x,y)\in\overline{\Gamma}, \tag{17}$$

where F_l is a function defined on $\overline{\Gamma}$ such that

$$\int_{\overline{\Gamma}}(h-b(x,y))\ F_l(t,x,y)\ dl=\int_\Omega\eta(t,x,y)\ dx\,dy,\quad \forall t\in\mathbb{R}. \tag{18}$$

For the sake of simplicity[1], we choose a function F_l constant in space: $F_l=F_l(t)$. Equation (18) becomes:

$$F_l(t)=\frac{\displaystyle\int_\Omega\eta(t,x,y)\ dx\,dy}{\displaystyle\int_{\overline{\Gamma}}(h-b(x,y))\ dl},\quad \forall t\in\mathbb{R}. \tag{19}$$

[1] More realistic numerical choices (such as a Poiseuille profile) have been done, but do not influence the solution properties.

Remark 2.2. *With such a definition of $F_l(t)$, the problem made of equation* (12) *and boundary conditions* (15) *and* (17) *has clearly a solution ψ as soon as b and η are regular enough. This solution is unique up to an additive constant; this non-uniqueness is not a real issue since the quantity of interest is the velocity $\vec{v} = \nabla\psi$.*

As a conclusion, the vector field of the water flow inside the lagoon may be computed by $\vec{v} = \nabla\psi$ where ψ is the solution to (12), (15), (17), and (19).

2.3 Equation for the confinement field

Having vector field $\vec{v} = (v_1, v_2)$ given by (6) on hand, it is obvious to see that a solution $\overline{g}$ of

$$\frac{\partial \overline{g}}{\partial \tau}(\tau, x, y) + \vec{v}(\tau, x, y) \cdot \nabla \overline{g}(\tau, x, y) = 0, \quad \forall \tau \in \mathbb{R},\ \forall (x, y) \in \Omega, \tag{20}$$

remains constant when following trajectories (X, Y) having velocity $\vec{v}(\tau, X, Y)$. To make this statement more precise, we define $X = X(\tau; x, y, s)$ and $Y = Y(\tau; x, y, s)$ as being the solution to the dynamical system

$$\begin{cases} \dfrac{\partial X}{\partial \tau}(\tau, x, y, s) = v_1(\tau, X(\tau; x, y, s), Y(\tau; x, y, s)), & X(s; x, y, s) = x, \\ \dfrac{\partial Y}{\partial \tau}(\tau, x, y, s) = v_2(\tau, X(\tau; x, y, s), Y(\tau; x, y, s)), & Y(s; x, y, s) = y. \end{cases} \tag{21}$$

It is then easy to verify that a solution $\overline{g}$ of (20) is such that

$$\begin{aligned} &\frac{\partial \left[\overline{g}(\tau, X(\tau; x, y, s), Y(\tau; x, y, s))\right]}{\partial \tau} = \frac{\partial \overline{g}}{\partial \tau}(\tau, X(\tau; x, y, s), Y(\tau; x, y, s)) \\ &+ \frac{\partial X}{\partial \tau}(\tau; x, y, s) \frac{\partial \overline{g}}{\partial x}(\tau, X(\tau; x, y, s), Y(\tau; x, y, s)) + \frac{\partial Y}{\partial \tau}(\tau; x, y, s) \frac{\partial \overline{g}}{\partial y}(\tau, X(\tau; x, y, s), Y(\tau; x, y, s)) \\ &= \frac{\partial \overline{g}}{\partial \tau}(\tau, X(\tau; x, y, s), Y(\tau; x, y, s)) \\ &+ \vec{v}(\tau, X(\tau; x, y, s), Y(\tau; x, y, s)) \cdot \nabla \overline{g}(\tau, X(\tau; x, y, s), Y(\tau; x, y, s)) = 0, \end{aligned} \tag{22}$$

meaning exactly

$$\overline{g}(\tau, X(\tau; x, y, s), Y(\tau; x, y, s)) \text{ is constant with respect to } \tau. \tag{23}$$

Property (23) means that a solution of (20) transports information with velocity given by $\vec{v}$. We will use this property to compute the confinement within the lagoon. The idea we follow consists in putting the correct information concerning time on the lagoon entrance, so that its transportation provides the value of the confinement in any point of the lagoon[2].
For any time $t > 0$ and given a sufficiently large time T, the solution $g_t = g_t(\tau, x, y)$ of

$$\begin{cases} \dfrac{\partial g_t}{\partial \tau}(\tau, x, y) + \vec{v}(t - T + \tau, x, y) \cdot \nabla g_t(\tau, x, y) = 0, & \forall 0 < \tau < T,\ \forall (x, y) \in \Omega, \\ g_t(\tau, x, y) = T - \tau, & \forall 0 < \tau < T,\ \forall (x, y) \in \overline{\Gamma}, \\ g_t(0, x, y) = T, & \forall (x, y) \in \Omega, \end{cases} \tag{24}$$

[2]For the sake of clarity, the corresponding computations are detailed in Appendix.

is such that $g_t(T,x,y)$ is the value of the instantaneous confinement (see Definition 2) at instant $t \in \mathbb{R}^+$ and position $(x,y) \in \Omega$. Indeed, if we consider a particle present at position $(x,y) \in \Omega$ at time $t > 0$, then this particle has travelled from the boundary $\overline{\Gamma}$ to its actual position during the time $g_t(T,x,y)$.

As a conclusion, solving (24) with a given value of T will give the confinement field in the part of the lagoon corresponding to a confinement smaller than T. Naturally, one has to take a sufficiently large T (for instance, 100 days in a small lagoon) to be sure that the confinement map will cover most of the domain.

2.4 Numerical simulation of the confinement with a constant evaporation rate

We start with the case where the evaporation rate η is a positive constant. Since there is no time dependancy, definitions 1, 2 and 3 coincide. In this case, the fluid velocity $\vec{v}$ and equation (24) are no more parametrized by t: $\vec{v}(t,x,y) = \vec{v}(x,y)$ and $g_t(\tau,x,y) = g(\tau,x,y)$.
The considered geometry is represented in Figure 3. The water height represents the difference between h (which is constant) and the bathymetry b, here given by the function

$$b(x,y) = 0.8\,\cos^2\left(\frac{\pi\sqrt{x^2+y^2}}{2}\right). \tag{25}$$

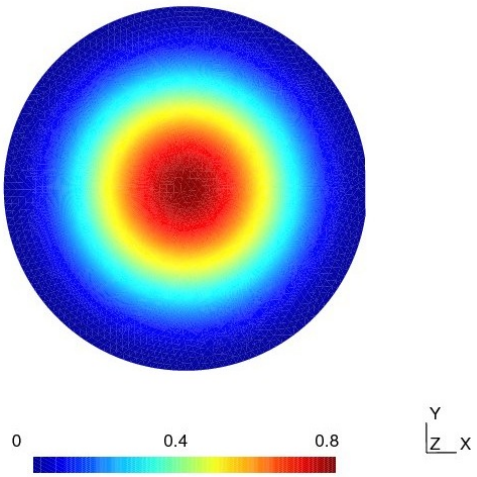

Figure 3: Circular lagoon with a flat eastern entrance, and isovalues of the bathymetry. The bathymetry corresponds to (25): its maximum level is reached at the lagoon center and it decreases towards the boundary.

As reported above, the velocity field does not depend on time: we plot it (together with its potential ψ) on Figure 4.

In this configuration, the confinement field is given in Figure 5.

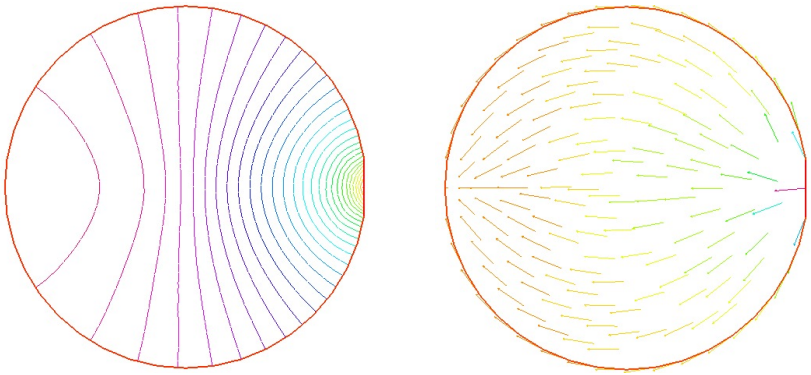

Figure 4: Isovalues of the velocity potential ψ (left) and corresponding vector field (right) for an evaporation rate $\eta = 1$. The isolines of the potential are orthogonal to the boundary Γ_0 thanks to the Neumann boundary condition (15). The vector field is orthogonal to the isolines of the potential, which can be anticipated since $\vec{v} = \nabla\psi$.

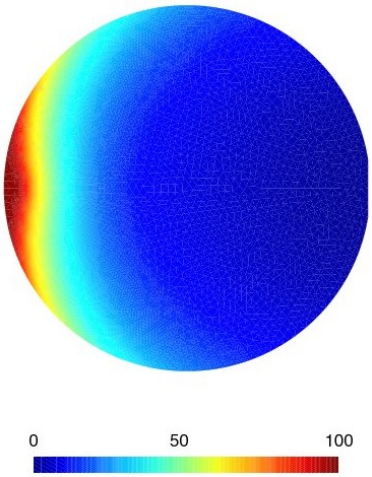

Figure 5: Confinement field for the bathymetry defined in (25) for a constant evaporation rate $\eta = 0.05$. A wide part of the lagoon is reached before $t = 50$, but the lagoon far end is much more confined.

2.5 Numerical simulation of the confinement with a uniform evaporation rate

In this paragraph we assume that η is space-independent, and is periodic in time with period $1/\omega$. From equations (12) and (6) we deduce that the vector field $\vec{v}$ is also $1/\omega$-periodic in time.
Finally, since in (24) the boundary conditions are independent of t, the function $t \mapsto g_t(\tau, x, y)$ is $1/\omega$-periodic. In this context, we will consider the effective confinement defined in Definition 3:

$$\langle g \rangle(T, x, y) = \omega \int_0^{1/\omega} g_t(T, x, y)\, dt. \tag{26}$$

The computational domain and the given bathymetry are identical to the previous simulations (see Figure 3). The velocity field is unstationnary, but one can easily check that

$$\vec{v}(\tau, x, y) = \eta(\tau)\, \vec{v}_{ref}(x, y), \tag{27}$$

where $\vec{v}_{ref}(x, y)$ is the reference velocity computed for $\eta = 1$ (see Figure 4). In this configuration, taking $\eta(\tau) = 1 + 0.9\cos(\tau)$, we plot in Figure 6 two instantaneous confinement fields.

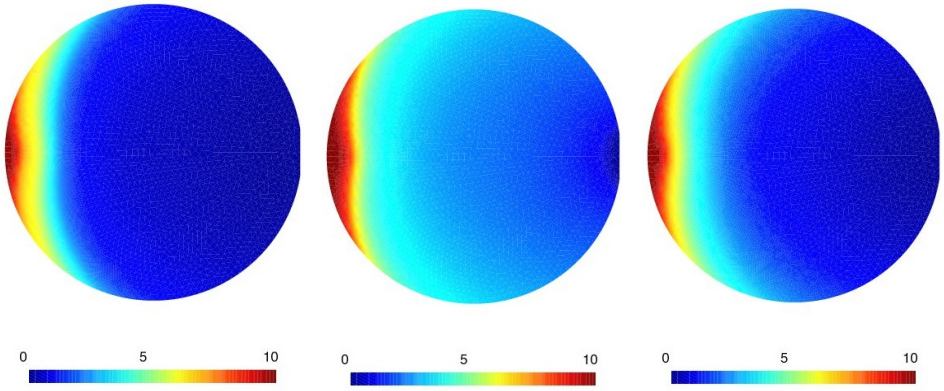

Figure 6: Instantaneous confinements at $t = t_1$ (left), and $t = t_2$ (middle) for a time-oscillating evaporation rate. Efficient confinement (right). Due to the time oscillation of the function η, the instantaneous confinements at different times t_1 and t_2 differ. The natural notion that comes to mind is thus the efficient confinement, computed thanks to (26).

Remark 2.3. *At this modelling level, we impose η to be non negative. Yet, in order to incorporate rains in the model, it could be interesting to consider that η may be negative at some times (so that the water flows out of the lagoon). Actually, we include this possibility in the coming section. Indeed, the model will account for tide oscillation, including periods where the water gets out of the domain.*

3 Model for confinement in a tide-submitted lagoon

Now, we improve the modeling procedure in order to account for a tide oscillation in the model. Notice that the resulting model accounts neither for seabed outcrop nor for foreshore.

3.1 Geometrical setting

The lagoon interior is the same cylinder based on $\Omega \subset \mathbb{R}^2$ as before (see Figure 2) with the supplementary assumption that the seabed function b is constant, with worth $\underline{b}$, on the lagoon interior entrance $\underline{\Gamma}$, making the lagoon interior entrance a rectangle. Because of the tide oscillation, the lagoon water mass is

inside the lagoon interior only at high tide of spring tide. Then, we consider a parallelepiped which horizontal lower face is called $\mathcal{R}$ (see Figure 2), having one of its vertical faces located at the lagoon interior entrance and long enough to collect the lagoon water mass at ebbing tide. The length of $\mathcal{R}$ is l and its width is γ. The considered domain is then $\tilde{\Omega} = \Omega \cup \mathcal{R}$ and the seabed is described by a continuous function $b : \tilde{\Omega} \to \mathbb{R}^+$, $b = b(x, y)$. For consistency with what follows, we assume that, on $\mathcal{R}$, b is constant with worth $\underline{b}$.

The water altitude is a function $h = h(t)$ such that

$$\inf_{t\in\mathbb{R}} h(t) = H - M \leq h(t) \leq H = \sup_{t\in\mathbb{R}} h(t), \tag{28}$$

where $H > M$ are such that $H - M > \sup_\Omega b$. The lagoon interior is then, at any time t,

$$\Big\{(x, y, z),\ (x, y) \in \Omega,\ b(x, y) < z < h(t)\Big\}, \tag{29}$$

and in order to locate the lagoon water mass at any time, we define a segment $\Gamma_m(t)$ parallel to the edge placed at the lagoon entrance, at a distance $\lambda(t)$ and joining the edges of $\mathcal{R}$, which is such that, defining $\mathcal{R}_m(t)$ by truncating $\mathcal{R}$ at $\Gamma_m(t)$,

$$\int_{\Omega\cup\mathcal{R}_m(t)\times[b(x,y),h(t)]} dx\,dy\,dz = \int_{\Omega\times[b(x,y),H]} dx\,dy\,dz. \tag{30}$$

This insures that the lagoon water mass occupies, at any time, a space of constant volume which is

$$\big(\Omega \cup \mathcal{R}_m(t)\big) \times [b(x, y), h(t)]. \tag{31}$$

Of course we require that $l \geq \max_{t\in\mathbb{R}} \lambda(t)$, which is achieved setting

$$l = \max_{t\in\mathbb{R}} \lambda(t) = \frac{1}{\gamma\underline{b}} M \int_\Omega dx\,dy. \tag{32}$$

3.2 Velocity field model

Clearly rising and ebbing tides induce a velocity field $\vec{V}(t, x, y)$ inside the lagoon water mass. We also consider $\vec{v}(t, x, y)$ the velocity field which is solely linked with the evaporation process (as in Section 2). Fields $\vec{V}$ and $\vec{v}$ are defined at all times on the moving domain $\Omega \cup \mathcal{R}_m(t)$.

Here, we set out an equation allowing the computation of both fields $\vec{V}$ and $\vec{v}$. We make similar assumptions on $\vec{v}$ and $\vec{V}$ as in Section 2: they are mean values of velocity over the vertical direction, they are purely horizontal and contain no vortex, so that:

$$\begin{cases} \vec{v}(t, x, y) = \nabla\psi(t, x, y), \\ \vec{V}(t, x, y) = \nabla\Psi(t, x, y), \end{cases} \qquad \forall t \in \mathbb{R}, \forall (x, y) \in \Omega \cup \mathcal{R}_m(t). \tag{33}$$

It is assumed that $\vec{v}$ is solely governed by the evaporation, while $\vec{V}$ solely induces variation of water altitude h.
To make this assumption precise, we consider a time interval $[t_1, t_2]$ with $t_1 < t_2$

and a regular subset $\mathcal{S}$ such that $\mathcal{S} \subset \Omega \cup \mathcal{R}_m(t)$ for any $t \in [t_1, t_2]$. The amount of water which enters the cylinder of basis $\mathcal{S}$ and with lateral area

$$\mathcal{L}(t) = \Big\{(x,y,z),\ (x,y) \in \partial\mathcal{S},\ b(x,y) < z < h(t)\Big\} \tag{34}$$

over $[t_1, t_2]$ is:

$$\begin{aligned} -\int_{t_1}^{t_2} \int_{\mathcal{L}(t)} \big(\vec{V}(t,x,y) + \vec{v}(t,x,y)\big) \cdot \vec{n}\ dl\, dz\, dt \quad = \\ -\int_{t_1}^{t_2} \int_{\partial\mathcal{S}} \big(h(t) - b(x,y)\big)\vec{V}(t,x,y) \cdot \vec{n}(x,y)\ dl\, dz\, dt \\ -\int_{t_1}^{t_2} \int_{\partial\mathcal{S}} \big(h(t) - b(x,y)\big)\vec{v}(t,x,y) \cdot \vec{n}(x,y)\ dl\, dz\, dt, \end{aligned} \tag{35}$$

where $\vec{n}$ has the same definition as in the previous section. What is precisely meant above is that the first term of the right-hand-side of (35) equals

$$\big(h(t_2) - h(t_1)\big) \int_{\mathcal{S}} dxdy = \int_{t_1}^{t_2} \int_S \frac{\partial h}{\partial t}(t)\ dx\, dy\, dt, \tag{36}$$

which is the volume variation over $[t_1, t_2]$ in the cylinder. The second term offsets the water quantity that evaporates through $\mathcal{S}$ over $[t_1, t_2]$ and which is

$$\int_{t_1}^{t_2} \Big(\int_S dx\, dy \Big) \eta(t)\, dt, \tag{37}$$

where we have assumed that the evaporation rate η is space independent.
Then, using the divergence operator $\nabla\cdot$ and formula (33), we finally get from the role distribution between $\vec{V}$ and $\vec{v}$ that

$$-\int_{t_1}^{t_2} \int_{\mathcal{S}} \nabla \cdot \Big[\big(h(t) - b(x,y)\big) \nabla\psi(t,x,y) \Big]\ dx\, dy\, dt \quad = \quad \int_{t_1}^{t_2} \Big(\int_S dx\, dy \Big) \eta(t)\, dt, \tag{38}$$

$$-\int_{t_1}^{t_2} \int_{\mathcal{S}} \nabla \cdot \Big[\big(h(t) - b(x,y)\big) \nabla\Psi(t,x,y) \Big]\ dx\, dy\, dt \quad = \quad \int_{t_1}^{t_2} \int_{\mathcal{S}} \frac{\partial h}{\partial t}(t,x,y)\ dx\, dy\, dt, \tag{39}$$

or

$$-\nabla \cdot \big[(h-b)\nabla\psi\big](t,x,y) \quad = \quad \eta(t), \quad \forall t \in \mathbb{R}\ \forall (x,y) \in \Omega \cup \mathcal{R}_m(t), \tag{40}$$

$$-\nabla \cdot \big[(h-b)\nabla\Psi\big](t,x,y) \quad = \quad \frac{\partial h}{\partial t}(t,x,y), \quad \forall t \in \mathbb{R}\ \forall (x,y) \in \Omega \cup \mathcal{R}_m(t), \tag{41}$$

Equations (40) and (41) must be provided with boundary conditions. Concerning (40), using the partition of $\partial(\Omega \cup \mathcal{R}_m(t))$, we set that no water enters the lagoon water mass through $\Gamma_0(t)$, yielding

$$\vec{v}(t,x,t) \cdot \vec{n}(t,x,y) = \frac{\partial\psi}{\partial\vec{n}}(t,x,y) = 0, \quad \forall t \in \mathbb{R},\ \forall (x,y) \in \Gamma_0(t). \tag{42}$$

We also set that at all times, the water entering the lagoon water mass through $\Gamma_m(t)$ exactly compensates for the evaporation through $\Omega \cup \mathcal{R}_m(t)$. This is translated into

$$\frac{\partial\psi}{\partial\vec{n}}(t,x,y) = f_m(t), \quad \forall t \in \mathbb{R},\ \forall (x,y) \in \Gamma_m(t), \tag{43}$$

where $f_m(t)$ is, for each t, a constant such that

$$-\int_{\Gamma_m}\big(h(t)-b(x,y)\big)\,f_m(t)\,dl=\int_{\Omega\cup\mathcal{R}_m(t)}\eta(t)\,dx\,dy. \tag{44}$$

Since $b\equiv 0$ on Γ_m, equation (44) reads:

$$f_m(t)=-\frac{\eta(t)}{\gamma h(t)}\int_{\Omega\cup\mathcal{R}_m(t)}dx\,dy=-\frac{\eta(t)}{\gamma h(t)}\big(|\Omega|+\gamma\lambda(t)\big), \tag{45}$$

where $\gamma=|\Gamma_m(t)|$ stands for the fairway's width.
Turning now to (41), we consider $\lambda'(t)$ the velocity of the moving boundary $\Gamma_m(t)$. Clearly $\vec{V}$ equals this velocity on $\Gamma_m(t)$. Hence, the boundary conditions for (41) are

$$\begin{cases}\dfrac{\partial\Psi}{\partial\vec{n}}(t,x,y)=\lambda'(t), \quad \forall t\in\mathbb{R}\ \forall(x,y)\in\Gamma_m(t),\\ \dfrac{\partial\Psi}{\partial\vec{n}}(t,x,y)=0, \quad \forall t\in\mathbb{R}\ \forall(x,y)\in\Gamma_0(t).\end{cases} \tag{46}$$

Remark 3.1. *There is a compatibility condition for the Laplace-Neumann problem constituted of equations* (41) *and* (46)*. This condition provides a differential equation for* $\lambda(t)$*, namely:*

$$h(t)\lambda'(t)+h'(t)\lambda(t)=-\frac{h'(t)}{\gamma}|\Omega|. \tag{47}$$

We now recall the two boundary-value problems that model the two velocities. For $\vec{v}=\nabla\psi$, we have

$$\begin{cases}-\nabla\cdot\big((h(t)-b)\nabla\psi\big)=\eta(t) \quad \text{on } \Omega\cup\mathcal{R}_m(t), & \text{(48a)}\\ \dfrac{\partial\psi}{\partial\vec{n}}=0 \quad \text{on } \Gamma_0, & \text{(48b)}\\ \dfrac{\partial\psi}{\partial\vec{n}}=f_m(t), \quad \text{on } \Gamma_m(t), & \text{(48c)}\end{cases}$$

and for $\vec{V}=\nabla\Psi$, the problem writes

$$\begin{cases}-\nabla\cdot\big((h(t)-b)\nabla\Psi\big)=h'(t) \quad \text{on } \Omega\cup\mathcal{R}_m(t), & \text{(49a)}\\ \dfrac{\partial\Psi}{\partial\vec{n}}=0 \quad \text{on } \Gamma_0, & \text{(49b)}\\ \dfrac{\partial\Psi}{\partial\vec{n}}=\lambda'(t) \quad \text{on } \Gamma_m(t). & \text{(49c)}\end{cases}$$

Remark 3.2. *Since we are interested in the total velocity* $\vec{v}+\vec{V}$*, we could now add the two contributions and set a system of PDEs for* $\vec{v}+\vec{V}$*. However, we think that for the sake of clarity, it is preferable to keep the systems separate. Naturally, the numerical computations can be done separately, or not.*

3.3 Domain decomposition for the velocity equations

Due to the particular shape of our computational domain, we will decompose it in two parts, namely Ω (which does not change with time), and the fairway $\mathcal{R}_m(t)$.
Indeed, in Ω we may use the same kind of computation as in Section 2, and in the moving fairway $\mathcal{R}_m(t)$ we will see that an explicit computation is possible, due to the simple (rectangular) geometry.

3.3.1 Equations for v

In the fixed domain Ω, the equations for ψ read:

$$\begin{cases} -\nabla \cdot \big((h(t)-b)\nabla\psi\big) = \eta(t) \quad \text{on } \Omega, & \text{(50a)} \\ \dfrac{\partial\psi}{\partial\vec{n}} = 0 \quad \text{on } \Gamma_0, & \text{(50b)} \\ \dfrac{\partial\psi}{\partial\vec{n}} = \underline{f}(t), \quad \text{on } \underline{\Gamma}, & \text{(50c)} \end{cases}$$

where $\underline{f}(t)$ is defined as

$$\underline{f}(t) = \frac{\eta(t)\,|\Omega|}{\gamma h(t)}. \tag{51}$$

In the moving domain $\mathcal{R}_m(t)$, we have for ψ (let us recall that $b \equiv 0$ in $\mathcal{R}_m(t)$):

$$\begin{cases} -\Delta\psi = \dfrac{\eta(t)}{h(t)} \quad \text{on } \Omega, & \text{(52a)} \\ \dfrac{\partial\psi}{\partial\vec{n}} = -\underline{f}(t) \quad \text{on } \underline{\Gamma}, & \text{(52b)} \\ \dfrac{\partial\psi}{\partial\vec{n}} = 0 \quad \text{on } \Gamma_0, & \text{(52c)} \\ \dfrac{\partial\psi}{\partial\vec{n}} = f_m(t), \quad \text{on } \Gamma_m(t), & \text{(52d)} \end{cases}$$

where f_m is defined in (45).
Actually, one can easily check that ψ does not depend on the space variable y and that we have in $\mathcal{R}_m(t)$:

$$v_1(x,y) = \frac{\partial\psi}{\partial x} = -\frac{\eta(t)}{h(t)}x + \underline{f}(t), \tag{53}$$

$$v_2(x,y) = \frac{\partial\psi}{\partial y} = 0. \tag{54}$$

Remark 3.3. *For the sake of simplicity, we have assumed that the interface $\underline{\Gamma}$ was located at the position $x = 0$.*

3.3.2 Equations for V

We have the same type of result for the other velocity contribution $\vec{V} = \nabla\Psi$:

$$\begin{cases} -\nabla \cdot \big((h(t)-b)\nabla\Psi\big) = h'(t) \quad \text{on } \Omega, & \text{(55a)} \\ \dfrac{\partial\Psi}{\partial\vec{n}} = 0 \quad \text{on } \Gamma_0, & \text{(55b)} \\ \dfrac{\partial\Psi}{\partial\vec{n}} = \underline{F}(t), \quad \text{on } \underline{\Gamma}. & \text{(55c)} \end{cases}$$

where $\underline{F}(t)$ is defined as

$$\underline{F}(t) = \frac{h'(t)\,|\Omega|}{\gamma h(t)}. \tag{56}$$

In the moving domain $\mathcal{R}_m(t)$ where $b \equiv 0$, we have for Ψ:

$$\begin{cases} -\Delta\Psi = \dfrac{h'(t)}{h(t)} \quad \text{on } \Omega, & \text{(57a)} \\ \dfrac{\partial\Psi}{\partial\vec{n}} = -\underline{F}(t) \quad \text{on } \underline{\Gamma}, & \text{(57b)} \\ \dfrac{\partial\Psi}{\partial\vec{n}} = 0 \quad \text{on } \Gamma_0, & \text{(57c)} \\ \dfrac{\partial\Psi}{\partial\vec{n}} = \lambda'(t), \quad \text{on } \Gamma_m(t), & \text{(57d)} \end{cases}$$

and one can easily check that Ψ does not depend on the space variable y either, and that we have in $\mathcal{R}_m(t)$:

$$V_1(x,y) = \frac{\partial\Psi}{\partial x} = -\frac{h'(t)}{h(t)}x + \underline{F}(t), \tag{58}$$

$$V_2(x,y) = \frac{\partial\Psi}{\partial y} = 0. \tag{59}$$

3.4 Confinement field model

Equipped with velocity fields $\vec{v}$ and $\vec{V}$, we now turn to the computation of the instantaneous confinement field at any time $t < T$, for a given (large) value of T, in any point of the lagoon water mass by solving:

$$\begin{cases} \dfrac{\partial g_t}{\partial\tau}(\tau,x,y) + \big(\vec{V}(t-T+\tau,x,y) + \vec{v}(t-T+\tau,x,y)\big)\cdot\nabla g_t(\tau,x,y) = 0, & \text{(60a)} \\ g_t(\tau,x,y) = T-\tau, \quad \forall 0<\tau<T,\ \forall (x,y)\in\Gamma_m(t-T+\tau), & \text{(60b)} \\ g_t(0,x,y) = T, \quad \forall (x,y)\in\Omega\cup\mathcal{R}_m(0). & \text{(60c)} \end{cases}$$

and by computing $g_t(T,x,y)$ at any point (x,y) where it is not greater than T.

Setting the condition (60b) on $\Gamma_m(t-T+\tau)$ is not an easy task since this condition holds on a moving boundary. Actually, we will extend the computational

domain from $\Omega \cup \mathcal{R}_m(t)$ to $\Omega \cup \mathcal{R}$ and impose the condition (60b) not only on $\Gamma_m(t - T + \tau)$ but also beyond this boundary:

$$g_t(\tau, x, y) = T - \tau, \quad \forall 0 < \tau < T \text{ and } \forall x \geq \lambda_m(t - T + \tau). \tag{61}$$

In order to satisfy (61) we will use a penalization term in equation (60a). This technique has been introduced in [ABF99] for the simulation of fluid flows with obstacles. We thus modify equation (60a) to obtain, in the new computational domain $\Omega \cup \mathcal{R}$,

$$\frac{\partial g_t}{\partial \tau}(\tau, x, y) + (\vec{V} + \vec{v})(t - T + \tau, x, y) \cdot \nabla g_t(\tau, x, y) + \frac{1}{\varepsilon}\big(g_t - (T - \tau)\big)\chi^m(t, x, y) = 0, \tag{62}$$

where ε is a positive number (to be chosen small), and $\chi^m(t, .)$ is the indicator function of $\overline{\mathcal{R} \backslash \mathcal{R}_m(t)}$:

$$\begin{cases} \chi^m(t, x, y) = 1, \forall (x, y) \in \overline{\mathcal{R} \backslash \mathcal{R}_m(t)}, \\ \chi^m(t, x, y) = 0, \forall (x, y) \in \Omega \cup \mathcal{R}_m(t), \end{cases}$$

Thanks to (62) and the definition of χ^m, one can immediately see that:

$$\begin{cases} \dfrac{\partial g_t}{\partial \tau}(\tau, x, y) + (\vec{V} + \vec{v})(t - T + \tau, x, y) \cdot \nabla g_t(\tau, x, y) = 0, \quad \forall (x, y) \in \Omega \cup \mathcal{R}_m(t), \\ g_t(\tau, x, y) = T - \tau + O(\varepsilon), \quad \forall (x, y) \notin \Omega \cup \mathcal{R}_m(t). \end{cases}$$

(64a)

(64b)

In particular, with this penalization method, equation (60a) holds in the moving domain $\Omega \cup \mathcal{R}_m(t)$, and the boundary condition (60b) is satisfied at order one in ε. The parameter ε will be chosen chosen small enough so that (64b) ia a good approximation of (60b).

3.5 Numerical results

We consider the same geometry for the computational domain as in Section 2. The circular lagoon Ω is supplemented with its entrance fairway, as in Figure 2, so that our numerical mesh corresponds to Figure 7.

In this domain, we compute the solution of the velocity equations (50) and (52) for the velocity $\vec{v}$ that corresponds to the water evaporation, together with the velocity equations (55) and (57) for the velocity $\vec{V}$ that corresponds to tidal oscillation. We have already mentioned (see Remark 3.2) that $\vec{v}$ and $\vec{V}$ could be either computed simultaneously or separately, which does not change the result. We also remind that solutions of equations (52) and (57) (in the fairway) can be computed explicitely (see (53) and (58)).

The total velocity field $\vec{v} + \vec{V}$ on hand, we can proceed to the computation of the confinement, which is done thanks to the computation of g_t solution of (60), or more precisely its penalized version (62).

We plot hereafter (see Figure 7) the total velocity field (left column) and the instantaneous confinement (right column) at different times. We draw the reader's attention on the fact that the flow may be entering the lagoon, or leaving it (see the velocity arrows). We end this section with the plot of the efficient confinement (see Figure 8), such as defined in 3.

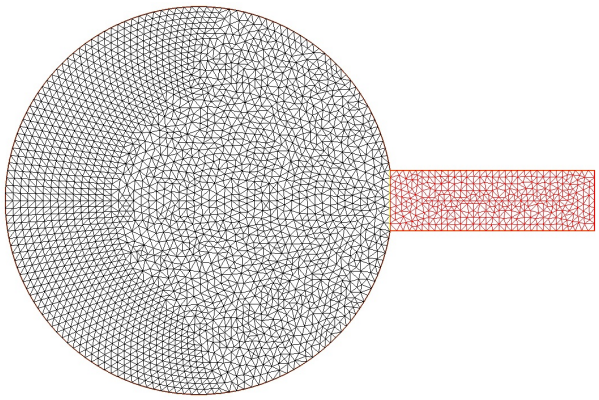

Figure 7: Discretization of the computational domain. Lagoon interior (black) and its fairway (red).

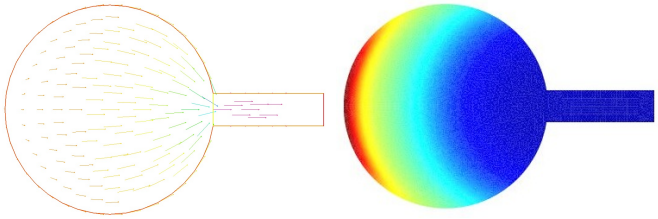

(a) $t = t_1$

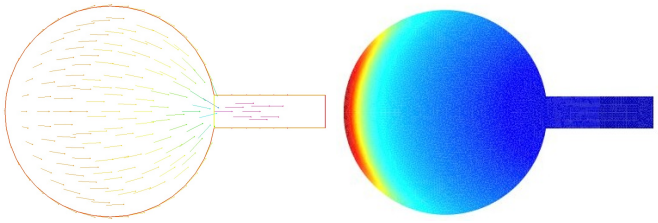

(b) $t = t_2$

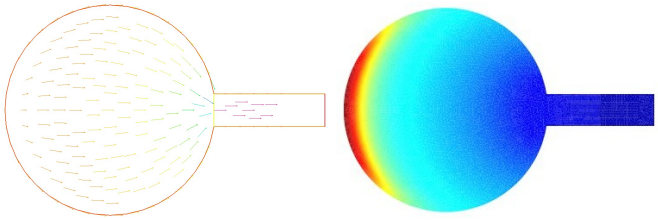

(c) $t = t_3$

4 Conclusion

In this paper, we improved a previously set out method to compute the confinement field within lagoons submitted or not submitted to tide. The model is based on a elliptic PDE to compute the water velocity field induced by evaporation (and by tide, if present) in the lagoon water mass and on a hyperbolic

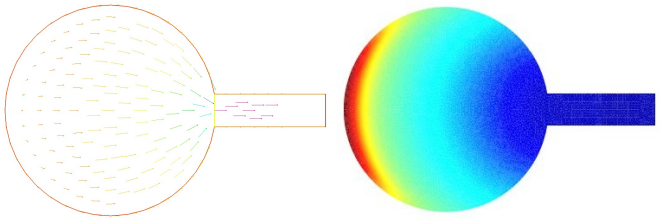

(d) $t = t_4$

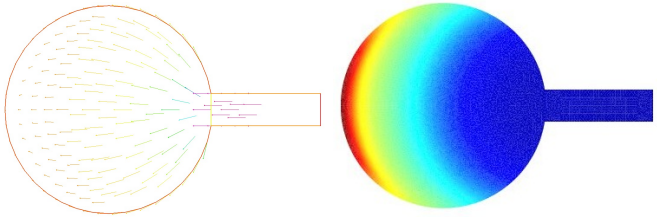

(e) $t = t_5$

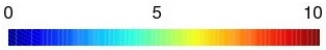

(f) Confinement levels

Figure 7: Velocity vector field (left column) and confinement field (right column) at various times. Depending on the snapshot, the flow may be entering or leaving the lagoon (mind the velocity arrows). The penalization parameter ε is set to 10^{-5}.

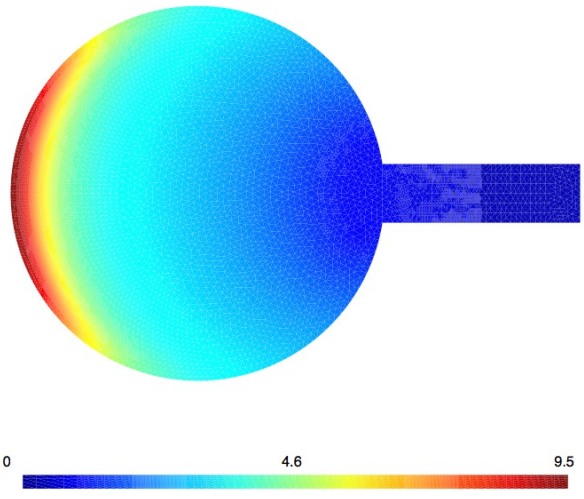

Figure 8: Effective confinement.

PDE to get the confinement. A code based on the Finite Element method was implemented using the FreeFem++ software environment. In the case of tide presence, where the model is set on a moving computational domain, we used a penalization method to insure dynamic boundary conditions. Our simulations

were performed in a simple (circular) lagoon, but this code allows to compute the confinement in a lagoon with any geometry, excluding seabed outcrops and foreshore.

Thanks to this new model, we will shortly perform numerical simulations in a real paralic environment for which we have bathymetry and mean currents data, together with informations on species distributions allowing comparisons with biological markers of confinement.
We also plan to study the multi-scales aspects of such models. On the one hand, we project to build a two-scale numerical method to simulate long term confinement evolution. On the other hand, we want to set a cascade of models, from the Mediterranean (closed) sea to small local lagoons; this includes the implementation of a dedicated software, accounting for several modelling scales and managing hierarchical data.

References

[ABF99] P Angot, CH Bruneau, and P Fabrie. A penalization method to take into account obstacles in incompressible viscous flows. *Numerische Mathematik*, 81(4):497–520, 1999.

[Bar94] Barnes. A critical appraisal of the application of Guélorget and Pertuisot's concept of the paralic ecosystem and confinement to macrotidal europe. *Estuarine, Coastal and Shelf Sciences*, 38:41–48, 1994.

[DPC93] J.-P. Debenay, J.-P. Perthuisot, and B. Colleuil. Expression numérique du confinement par les peuplements de foraminifères. app. aux domaines paral. actuels afri. w. *C. R. Acad. Sci., Paris, série II*, 316(2):1823–1830, 1993.

[FG07] E. Frénod and E. Goubert. A first step towards modelling confinement of paralic ecosystems. *Ecological Modelling*, 200(1-2):139–148, jan 2007.

[GFP83] O. Guélorget, G. F. Frisoni, and J.-P. Perthuisot. La zonation biologique des milieux lagunaires : définition d'une échelle de confinement dans le domaine paralique méditérranéen. *Journal de Recherche Océanographique*, 8:15–36, 1983.

[GGLP90] O. Guélorget, D. Gaujous, M. Louis, and J.-P. Perthuisot. Macrobenthofauna of lagoons in guadaloupean mangroves (lesser antilles) : role and expression of confinement. *Journal of Coastal Research*, 6:611–626, 1990.

[GP83a] O. Guélorget and J.-P. Perthuisot. Le confinement, paramètre essentiel de la dynamique biologique du domaine paralique. *Sciences Géologiques, Bulletin*, 14:25–34, 1983.

[GP83b] O. Guélorget and J.-P. Perthuisot. Le domaine paralique. Expressions géologiques biologique, et économique du confinement. Presse de l'école normale supérieure 16-1983, 45 rue d'Ulm, Paris, 1983.

[HPLH04] F. Hecht, O. Pironneau, and A. Le Hyaric. FreeFem++ manual. 2004.

[IGF+85] A. Ibrahim, O. Guélorget, G. G. Frisoni, J. M. Rouchy, A. Martin, and J.-P. Perthuisot. Expressions hydrochimiques, biologiques et sédimentologiques des gradients de confinement dans la lagune de guemsah (golfe de suez, egypte). *Oceanologica Acta*, 8:303–320., 1985.

[RD96] F. Redois and J.-P. Debenay. Influence du confinement sur la répartition des foraminifères benthiques : exemples de l'estran d'une ria mésotidale de Bretagne méridionale. *Revue de Paléobiologie*, 15(1):243–260, 1996.

[TSG09] D. Tagliapietra, M. Sigovini, and V. Ghirardini. A review of terms and definitions to categorise estuaries, lagoons and associated environments. *Marine and Freshwater Research*, 60(6):497–509, 2009.

Appendix: equation for the confinement

In this appendix we explain why, for any time $t > 0$ and given a sufficiently large time T, the solution $g_t = g_t(\tau, x, y)$ of

$$\begin{cases} \frac{\partial g_t}{\partial \tau}(\tau, x, y) + \vec{v}(t - T + \tau, x, y) \cdot \nabla g_t(\tau, x, y) = 0, & \forall 0 < \tau < T,\ \forall (x, y) \in \Omega, \\ g_t(\tau, x, y) = T - \tau, & \forall 0 < \tau < T,\ \forall (x, y) \in \overline{\Gamma}, \\ g_t(0, x, y) = T, & \forall (x, y) \in \Omega, \end{cases} \tag{65}$$

is such that $g_t(T, x, y)$ is the value of the instantaneous confinement (see Definition 2) at instant $t \in \mathbb{R}^+$ and position $(x, y) \in \Omega$. It is indeed the case since the value $g_t(\tau, x, y)$ of g_t at time τ and in position $(x, y) \in \Omega$ is either the value of the initial data (*i.e.* T) or the value of g_t on $\overline{\Gamma}$ at a former time. For $(x_0, y_0) \in \overline{\Gamma}$, we consider the characteristic $(\tilde{X}(\tau, x_0, y_0, 0), \tilde{Y}(\tau, x_0, y_0, 0))$ which is such that its origin

$$\big(\tilde{X}(0, x_0, y_0, 0), \tilde{Y}(0, x_0, y_0, 0)\big) = (x_0, y_0) \in \overline{\Gamma}, \tag{66}$$

passing by (x, y). This means that, for a given $\tau^* = \tau^*(t, x, y)$, we have

$$\big(\tilde{X}(\tau^*, x_0, y_0, 0), \tilde{Y}(\tau^*, x_0, y_0, 0)\big) = (x, y) \tag{67}$$

and that it is solution to

$$\begin{cases} \frac{\partial \tilde{X}}{\partial \tau}(\tau, x, y, s) = v_1(\tau - T + t, \tilde{X}(\tau; x, y, s), \tilde{Y}(\tau; x, y, s)), \\ \frac{\partial \tilde{Y}}{\partial \tau}(\tau, x, y, s) = v_2(\tau - T + t, \tilde{X}(\tau; x, y, s), \tilde{Y}(\tau; x, y, s)). \end{cases} \tag{68}$$

Notice that $\tau^* = \tau^*(t, x, y)$ is the time for the characteristic to go from the border $\overline{\Gamma}$ to (x, y) when (x, y) is reached at time t. Hence it is, by definition, the value of the instantaneous confinement in (x, y) at time t.
Beside this, reasoning like in paragraph 2.3, we get that g remains constant along the characteristics $(\tilde{X}, \tilde{Y})$ meaning

$$\begin{aligned} g_t(T, x, y) &= g_t(T, \tilde{X}(\tau^*, x_0, y_0, 0), \tilde{Y}(\tau^*, x_0, y_0, 0)) \\ &= g_t(T - \tau^*, \tilde{X}(0, x_0, y_0, 0), \tilde{Y}(0, x_0, y_0, 0)) \\ &= g_t(T - \tau^*, x_0, y_0) \\ &= T - (T - \tau^*) \\ &= \tau^*(x, y), \end{aligned} \tag{69}$$

i.e. the instantaneous confinement value in position (x, y) and time t. In order to get the ultimate equality in (69), we used (65).

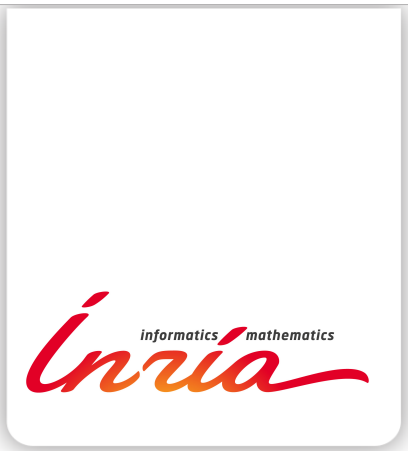

RESEARCH CENTRE
GRENOBLE – RHÔNE-ALPES

Inovallée
655 avenue de l'Europe Montbonnot
38334 Saint Ismier Cedex

Publisher
Inria
Domaine de Voluceau - Rocquencourt
BP 105 - 78153 Le Chesnay Cedex
inria.fr

ISSN 0249-6399